Published in IET Renewable Power Generation
Received on 15th July 2008
Revised on 6th October 2008
doi: 10.1049/iet-rpg:20080065

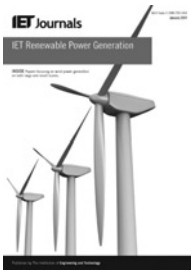

ISSN 1752-1416

Artificial neural network-polar coordinated fuzzy controller based maximum power point tracking control under partially shaded conditions

Syafaruddin[1] *E. Karatepe*[2] *T. Hiyama*[1]

[1]*Department of Computer Science and Electrical Engineering, Kumamoto University, 2-39-1 Kurokami, Kumamoto 860-8555, Japan*
[2]*Department of Electrical and Electronics Engineering, Ege University, 35100 Bornova-Izmir, Turkey*
E-mail: syafa@st.eecs.kumamoto-u.ac.jp

Abstract: The one of main causes of reducing energy yield of photovoltaic systems is partially shaded conditions. Although the conventional maximum power point tracking (MPPT) control algorithms operate well under uniform insolation, they do not operate well in non-uniform insolation. The non-uniform conditions cause multiple local maximum power points on the power–voltage curve. The conventional MPPT methods cannot distinguish between the global and local peaks. Since the global maximum power point (MPP) may change within a large voltage window and also its position depends on shading patterns, it is very difficult to recognise the global operating point under partially shaded conditions. In this paper, a novel MPPT system is proposed for partially shaded PV array using artificial neural network (ANN) and fuzzy logic with polar information controller. The ANN with three layer feed-forward is trained once for several partially shaded conditions to determine the global MPP voltage. The fuzzy logic with polar information controller uses the global MPP voltage as a reference voltage to generate the required control signal for the power converter. Another objective of this study is to determine the estimated maximum power and energy generation of PV system through the same ANN structure. The effectiveness of the proposed method is demonstrated under the experimental real-time simulation technique based dSPACE real-time interface system for different interconnected PV arrays such as series-parallel, bridge link and total cross tied configurations.

1 Introduction

The output characteristic of a photovoltaic (PV) array is changed depending on solar irradiance, temperature, mismatched cells, partially shaded conditions and array configuration. Non-uniform insolation conditions are sometimes inevitable in a PV power system because some parts of the module or array receive less intensity of sunlight because of the utility poles, trees, chimneys or parts of other buildings and dirt on the module's top surface. The partially cloudy conditions also cause unpredictable non-uniform insolation conditions. In recent years, PV power generation systems have been used in private residences and PV modules are normally installed on the roof. The chimneys of building may cause significant shading on PV array [1]. Non-uniform insolations cause differences in current–voltage (I–V) characteristics and the power–voltage (P–V) characteristics obtain more complicated with multi-local maximum power point (MPP). In these reasons, tracking the MPP is difficult under the partially shading or non-uniform conditions. To achieve highest possible performance of PV conversion and cover the high cost of solar cells, maximum power point tracking (MPPT) controller is an essential part of PV system [2]. Therefore, suitable MPPT control systems must be developed for all environmental

conditions, especially for partial shaded conditions and the investigations of mismatching effects must be increased for improving the performance and reliability of PV systems.

Several MPPT control algorithms have been studied so far. They can be classified according to MPPT algorithms such as constant voltage control, perturbation and observation, incremental conductance and current feedback algorithms [2, 3]. Most of them have been developed for uniform insolation conditions. If there are multiple peak points due to the partially shading and other mismatching effects, the conventional MPPT control algorithms are not useful and converge to a local MPP [2, 4, 5]. However, the conventional algorithms operate very well under the uniform insolation conditions. But they cannot distinguish between the global and local peaks since local MPP shows the same typical characteristics as global MPP, such as it has $dP/dV = 0$ and the slope at its right and left sides have different signs. Thus, an amount of power generation can not be utilised by using conventional algorithms when partially shaded occurs or some parts of PV array are damaged [2, 6]. As a result, in recent years, there are significant efforts to reduce this kind of mismatching losses [7–13].

Shimizu *et al* [7] proposed the operation voltage control circuit where dc–dc converter is installed in each module. However, this method might result in excessive complexity of the system configuration. Furthermore, the controlling operation of that system has some limitations and causes power losses with associated power conversion stages. Mishima and Ohnishi [8] proposed a system with output power control of array on a PV string basis which provides to be more efficient and simpler way in the PV power compensation for non-uniform insolation conditions. Kobayashi *et al.* [9] and Irisawa *et al.* [10] proposed two sequential stages of MPPT control system. The first stage of control drives the operating point of PV system to the near global peak point and forces to converge to this point in the second stage. However, this method is only powerful on some non-uniform insolation conditions. For this reason, it requires some additional control process to track the real MPP. Ahmed and Miyatake [11] proposed a MPPT employing a line search algorithm with improved Fibonacci search to find the global MPP when the PV array is partially shaded. Patel and Agarwal [12] used Matlab-based modelling to show the partially shaded effects and reference [13] presented critical observations that are useful for global MPP tracking and an algorithm for tracking the global peak. All the efforts for overcoming the partially shaded problems show that advanced MPPT systems should be developed and the investigation of finding optimal solutions should be increased to obtain more reliable PV system.

In this paper, a novel voltage based MPPT system is proposed for partially shading conditions. The main part of the proposed system is to determine the global MPP voltage of PV array for different partially shaded conditions. Since there are several non-uniform insolation conditions and corresponding complicated $P–V$ characteristics, it is very difficult to determine that which peak is the global MPP by using the conventional methods. The location of global peak is strongly dependent of shading pattern [4, 12, 13]. An artificial neural network (ANN) is accepted as a technology offering an alternative way to solve this kind of complex problems. In this study, the ANN is trained by observing several partially shaded conditions and the global MPP voltage is estimated very quickly without using complexity algorithms and techniques. Since it is very difficult to follow the shifting of global MPP under the partially shaded condition, estimation of global MPP voltage in time as a reference signal for power converter is one of the solutions to improve the performance of MPPT simply. In this paper, polar coordinated fuzzy controller is used for power converter. The fuzzy logic controller model has been used and quite attractive results are achieved in the power system stabilisers (PSS) application [14]. However, this type of fuzzy logic controller is first applied for the MPPT control of PV applications. The fuzzy logic with polar information controller generates control signal for the power converter simply. The main advantage of fuzzy logic controller is that the accurate description of the system to be controlled is not required and there are not wide parameter variations with respect to the standard regulators.

The state of the art techniques increase the complexity and cost of the system. However, on the other hand, the reliability of MPPT control of PV system under all environmental conditions is very important issue for PV systems to become confiding energy sources in urban areas. Also, different array configurations instead of using simple series-parallel (SP) connection are an alternative method to reduce the non-uniform insolation effects [15]. These configurations are called as bridge link (BL) and total cross tied (TCT) connections. Finally, the effectiveness of the proposed MPPT system is tested through developed experimental real-time simulator for different interconnected configurations on daily basis of irradiance conditions.

The estimation of available energy for unpredictable operating conditions is another important point in the stand-alone or hybrid systems. Daily, monthly and yearly predictions are very important for the planning operation of the entire power systems and market-pricing decisions, especially under partially shaded conditions. In the stand-alone and hybrid systems, the estimated maximum output power is very useful for optimising the operating condition of equipments, such as battery, inverter and charger controller [16, 17]. Moreover, the scheduling of other generation units in hybrid systems can be precisely determined for the sake of supply reliability and reduction in the investment cost [16, 18]. Meanwhile, the estimated output energy of PV system as the continuous

doi: 10.1049/iet-rpg:20080065

measurements of power generation prediction will be beneficial to the investment calculation of solar energy system [19]. The estimated output power and generation capacity of PV system had been presented in some papers [20–22]. In [20], the TRNSYS simulation software was used to predict the overall performance of PV systems, such as PV and inverter efficiency and overall system efficiency in the long term performance. Monte Carlo simulation method was applied to assess the adequacy of generation capability of small stand-alone power systems containing solar energy because of the chronological random nature of the solar irradiance level and the dependencies associated with the site location of PV units [21]. Meanwhile, the ANN has been applied to estimate the maximum power generation from PV module using environmental information [22]. In this paper, the proposed system is used to estimate the available optimum energy of a PV array under both uniform and non-uniform insolation conditions by using the same ANN process.

2 Configuration of the proposed system

The configuration of proposed system consists of PV array, ANN, fuzzy logic controller and converter as shown in Fig. 1. The input signals for the PV array are the irradiance level (E) in W/m^2 and the cell temperature (T_c) in degree Celsius, whereas the actual voltage and power expressed in V_{dc} and P_{dc}. The neural network is trained to predict the global MPP voltage (V^*_{dc}) and power (P^*_{dc}) by observing through P–V curves for different partially shaded conditions as a function of E and T_c. The optimum output voltage (V^*_{dc}) is required as a reference signal for the voltage based MPPT controller. At the same time, the global maximum power (P^*_{dc}) is used to calculate the available optimum output energy of PV array. The difference between the V_{dc} and the V^*_{dc}, which denoted with error (e) together with tuning parameters of A_s and D_r are used as inputs for the fuzzy logic controller in order to produce the control signal U_c. This control signal is used to adjust the duty ratio of buck converter. Power converter is low cost, simple and high efficiency unit in MPPT of PV applications. Further details on the configuration of the proposed system will be explained in the following sections.

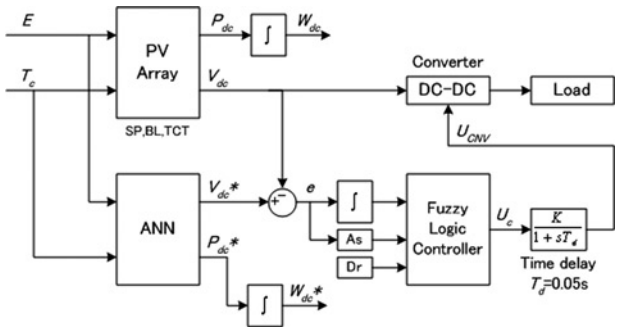

Figure 1 *Configuration of proposed system*

2.1 PV array configurations

Two different size PV array, one of size is 3 × 3 and the other of size is 20 × 3 are used to test the reliability of proposed system. Three interconnection schemes, SP, BL and TCT are considered for both sizes to compare the PV array configurations as shown in Fig. 2. The PV arrays comprise SM 55 PV modules [23]. The electrical specification of this module under standard test condition (STC) can be seen in Table 1.

When the modules are connected in series, the shaded modules force to change the optimum operating point of non-shaded modules [4]. With adding extra wires in the module connections, such as in BL and TCT configurations, new current paths are created and the output PV power can be increased under the non-uniform insolation conditions. However, this kind of connections can be useful under some shading patterns [15]. Therefore, they alone can not be sufficient solution for partially shaded problem.

SM-55 PV module comprises 36 series connected mono-crystalline silicon cells and two bypass diodes [15, 24]. The first bypass diode is connected in terminal of the 1st cell to 18th cell, whereas the other one is connected in the terminal of remaining cells. The nature characteristics of PV modules under shading conditions when bypass diodes connected in module terminal are explained as follows. Under partially shaded condition, the shaded cells become reverse bias and behave as a load instead of generator that leads to the hot spot problem. To avoid hot spot effect, bypass diode is deployed to drive the current of the non-shaded parts. However, the connection of bypass diodes will change the uniform I–V and P–V characteristics of the module, resulting in multiple peaks. In [25], two kinds of bypass diode connections are introduced based on the manufacturer recommendation, called overlapped and non-overlapped cells. The deformation of module I–V characteristics is bigger when the shaded parts show low slope in reverse bias condition until the bypass diode starts to conduct. Regarding the bypass diode connection type, the shaded parts can cause to force the optimum operating voltage to abnormally low-voltage region on the I–V curve. From this view point, the non-linear characteristic of I–V curve can mislead the inverter in searching the MPP and the inverter cannot distinguish between global and local MPPs. Series connected PV modules are normally carrying the same current. However, it is not all the case, and then the bypass diode is connected to allow the current of non-shaded parts flowing in bypass diode of shaded modules [26]. Once a bypass diode is activated, the operating voltage will change to be low in the P–V curve. To illustrate the bypass diode effect, the comparison of P–V curves of 3 × 3 PV array with and without bypass diodes under the partially shaded condition is given in Fig. 3. The voltage and power at MPP under non-shaded condition which is specified at 1000 W/m^2, 25°C are about 52 V

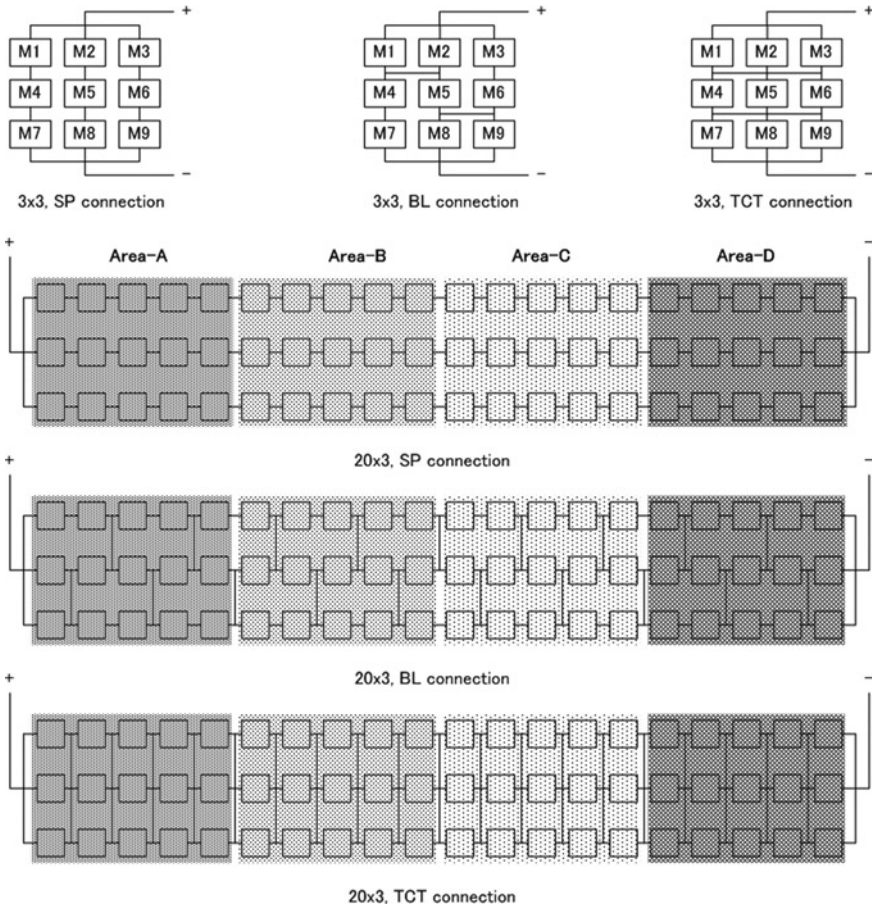

Figure 2 *SP, BL and TCT PV array connections for 3 × 3 and 20 × 3 PV array*

and 493 W, respectively. If the bypass diode is not used and the irradiation of some parts of modules is reduced to 100 W/m^2, the output power decreases to a serious level. When the bypass diode is used, multiple MPP is observed. In that case, the global MPP voltage and power are 15.9 V and 149.9 W, respectively. Without bypass diode, only one MPP will occur where the voltage is remained at 53 V, but the MPP power is limited to about 52 W. In that respect, bypass diode has two functions. The one of them is to prevent the hot spot effect and the other one is giving an opportunity to obtain more power from the PV array under the partially shaded conditions if a convenient MPPT method can be used.

Table 1 Specification of SM 55 PV module for standard test conditions AM 1.5, 1000 W/m^2, 25°C

maximum power	55 W
open circuit voltage	21.7 V
short circuit current	3.45 A
voltage at maximum power point	17.4 V
current at maximum power point	3.15 A

In this paper, two different irradiance profiles which are based on the daily measurement from 6 a.m. to 6 p.m. are used as shown in Fig. 4. In Fig. 4*a*, the pattern is considered for slowly changing condition, whereas Fig. 4*b* is for rapidly changing condition. Normally, irradiance level can be monitored in each module by pyranometer set. However, to reduce the cost of the system, the silicon solar cells are used

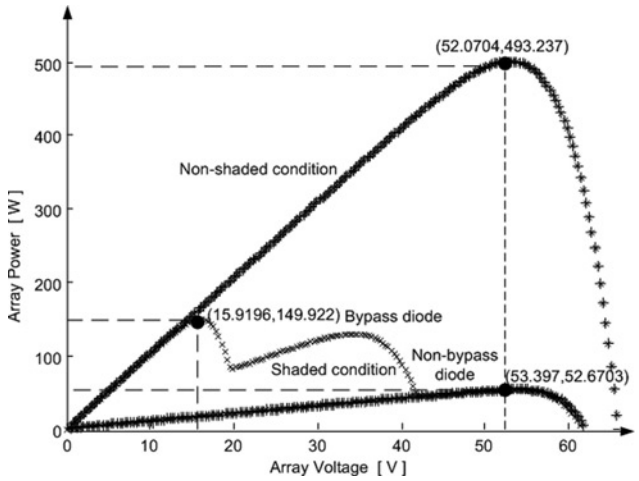

Figure 3 *P–V curve in shaded and non-shaded operations for 3 × 3 PV array*

doi: 10.1049/iet-rpg:20080065

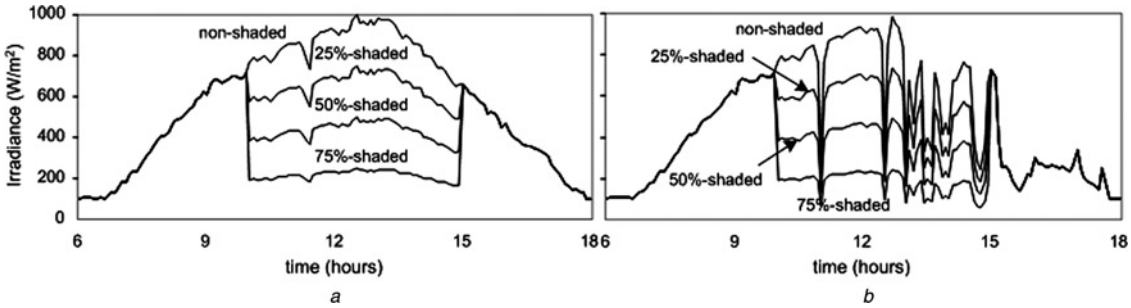

Figure 4 *Daily basis of irradiance measurement*

a Slow changes in irradiance
b Rapid changes in irradiance

instead of pyranometer to measure the incoming irradiance level for each module. A silicon solar cell can be used as an irradiance sensor, because the short-circuit current is proportional to irradiance [27, 28]. The cell temperature is predetermined to be constant at 50°C, for the reason that the cell temperature will raise to high level beyond the ambient temperature and it changes very slowly in daily operation of PV array.

2.2 ANN based estimated optimum voltage and power of PV array

Recently, the application of ANN has entered various engineering fields as an estimation method due to the high pattern recognition ability. Moreover, the ANN can offer benefits such as no requirement for knowledge on internal system parameters, requires less computational effort and provides a compact solution for multivariable problems [15]. Several shading patterns are arbitrarily specified during the training process of the ANN. In this paper, a three layer feed-forward neural network is used: an input, a hidden and an output layer to estimate MPP voltage and power of PV array. To reduce the computational efforts, instead of using the irradiance of all PV modules, only a few input signals which are specified. For 3 × 3 PV array, the average of irradiance of selected modules as expressed as follows:

$$E_1 = 0.25 \times (E_{M1} + E_{M2} + E_{M4} + E_{M5}) \quad (1)$$

$$E_2 = 0.25 \times (E_{M2} + E_{M3} + E_{M5} + E_{M6}) \quad (2)$$

$$E_3 = 0.25 \times (E_{M4} + E_{M5} + E_{M7} + E_{M8}) \quad (3)$$

$$E_4 = 0.25 \times (E_{M5} + E_{M6} + E_{M8} + E_{M9}) \quad (4)$$

where E_1, E_2, E_3 and E_4 are the average of incoming irradiance level on group of modules (M1, M2, M4, M5), (M2, M3, M5, M6), (M4, M5, M7, M8) and (M5, M6, M8, M9), respectively. The configuration of proposed ANN can be seen in Fig. 5.

Following a similar selection method for the input signals of the ANN in 3 × 3 PV arrays where every sensors measure the average of incoming irradiance on the 4 adjacent modules, the number of input signals for 20 × 3 PV array will end up with 38 input signals. In this large size of PV system, the global and local MPP voltages are almost same if lightly shaded or the shade covers only a few modules. It means that conventional MPP algorithm can find the global MPP without using complex method. In that reason, 20 × 3 PV array is partially shaded in terms of four parts (A, B, C and D) as shown in Fig. 2 in order to investigate the proposed system under heavily shaded conditions. Shadowing the area of A, B, C and D regions with different insolations are merely intended to show that the proposed controller is able to follow the shifting of optimum MPP voltage. From these facts, the three layer feed-forward neural network is enough to map between shading patterns and MPP voltage and power for small size (3 × 3) and large size (20 × 3) PV arrays. The experimental results will be given in the following sections.

In the hidden layer, the sigmoid function is utilised for the input-output characteristics of the nodes. For each node i in the hidden and output layers, the output $O_i(k)$ is given as follows

$$O_i(k) = \frac{1}{1 + e^{-I_i(k)}} \quad (5)$$

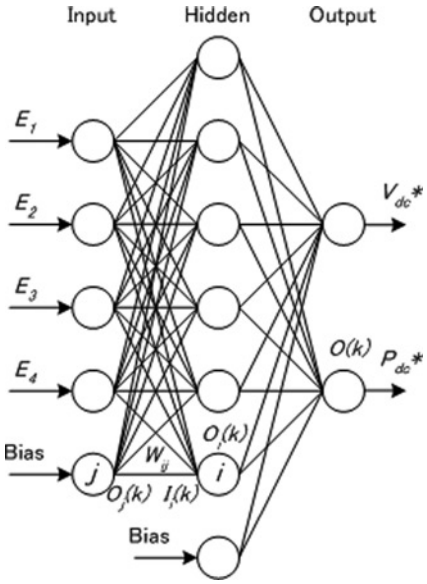

Figure 5 *Proposed configuration of ANN*

The term $I_i(k)$ in (5) is the input signal to node i at the kth sampling. The input $I_i(k)$ is given by the weighted sum of the input nodes as follows

$$I_i(k) = \sum_j w_{ij}(k) O_j(k) \tag{6}$$

where w_{ij} is the connection weight from node j to node i and $O_j(k)$ is the output from node j.

To identify the optimum voltage and output power accurately, the connection weights w_{ij} must be calculated by using typical patterns called the training process. In the training process, a set of input–output patterns for neural network is required. During the training, the connection weights w_{ij} are modified recursively until the best fit is achieved for the input–output patterns based on the minimum value of the sum of the squared errors. The equation of the sum of squared errors (SSE) is described as:

$$\text{SSE} = \sum_{k=1}^{N} (t(k) - O(k))^2 \tag{7}$$

where N is the total number of training patterns, $t(k)$ the kth target output from the output node and $O(k)$ the computed value. Initially, the value of connection weights w_{ij} is set to random values. For all the training patterns, the error function is evaluated and the connection weights w_{ij} are updated to minimise the error in (7).

There are about 370 shading patterns for the training process for 3 × 3 PV array, include the uniform insolation conditions between 100 and 1000 W/m^2 explained in Table 2. The similar process is applied for 20 × 3 PV array. During the training process, the learning rate and the momentum are specified to 0.2 and 0.85, respectively [29].

Table 2 Criteria selection for the input–output training data set

Base irradiance (W/m^2)	Pre-determined shading on selected modules (W/m^2)
200	100
300	100, 200
400	100, 200, 300
500	100, 200, 300, 400
600	100, 200, 300, 400, 500
700	100, 200, 300, 400, 500, 600
800	100, 200, 300, 400, 500, 600, 700
900	100, 200, 300, 400, 500, 600, 700, 800
1000	100, 200, 300, 400, 500, 600, 700, 800, 900

The number of hidden nodes is determined based on the total minimum errors during the training process. The minimum of the SSE in the training process for SP, BL and TCT connections of 3 × 3 PV array is achieved around 0.0253 when the number of hidden nodes is 12. For 20 × 3 PV array, the minimum of SSE and the number of hidden nodes are obtained at 0.0335 and 44, respectively.

A performance index (J) is defined to verify the training results between the optimum and the target values for all PV array connections, expressed as follows. The smallest values of both J_V and J_P are expected in this case that indicates how close the values between the optimum and the target. In this study, the maximum power point (MPP) voltage (V_{mp}) and power (P_{mp}) which are observed through P–V curve for different shading conditions are used as the target outputs, whereas V^*_{dc} and P^*_{dc} are the optimum voltage and power, respectively.

$$J_V = \int (V^*_{dc} - V_{mp})^2 \, dt \tag{8}$$

$$J_P = \int (P^*_{dc} - P_{mp})^2 \, dt \tag{9}$$

These performance indexes are calculated with the different partially shaded patterns by using three different set of weights. The overall index results for 3 × 3 and 20 × 3 PV arrays are shown in Table 3. These results show that the prediction of global MPP voltage as a reference signal for controller is one of the solutions to reduce the power losses of partially shaded PV array.

2.3 Fuzzy logic schemes for MPPT control of PV system under partially shaded condition

In this section, a fuzzy logic control scheme with polar information is described for the MPPT control of PV system under partially shaded condition. Similar fuzzy logic rules are already used in PSS application [14]. Fuzzy logic controller has three important stages as rule base, fuzzification and defuzzification. As shown in Fig. 6, there are seven fuzzy levels are used for high accuracy, such as NB (negative big), NM (negative medium), NS (negative small), Z (zero), PS (positive small), PM (positive medium) and PB (positive big). In this table, the Z (zero) diagonal represents the switching line where divides the tables into two parts of control actions. Above the switching line contains negative signals for deceleration control action, although under the switching line provides positive signals as acceleration control action.

The fuzzy rule assignment table which represents the rule base, then transformed into the phase plane as shown in Fig. 7. The sectors A in the first quadrant and B in the third quadrant are defined as the maximum control actions for deceleration and acceleration, respectively. Meanwhile,

doi: 10.1049/iet-rpg:20080065

Table 3 Overall performance index in the ANN training process for 3 × 3 and 20 × 3 PV arrays

Irradiance	PV array		Non-shaded		25%-shaded		50%-shaded		75%-shaded	
			J_V	J_P	J_V	J_P	J_V	J_P	J_V	J_P
Slow changes	3 × 3	SP	0.247	5.975	0.509	16.303	1.395	19.628	9.076	19.191
		BL	0.247	5.975	0.266	19.533	0.550	12.220	0.951	10.573
		TCT	0.247	5.975	0.269	5.757	0.463	9.876	0.448	4.709
Rapid changes		SP	1.029	5.295	4.158	14.945	8.031	50.693	11.098	49.350
		BL	1.029	5.295	2.458	15.659	6.180	19.025	7.335	39.696
		TCT	1.029	5.295	1.250	6.280	4.185	10.148	2.691	10.962
Slow changes	20 × 3	SP	0.338	7.853	0.618	15.306	3.467	22.346	11.257	22.346
		BL	0.338	7.853	0.457	20.654	1.457	13.578	1.897	11.254
		TCT	0.338	7.853	0.358	9.798	2.437	11.259	1.574	8.875
Rapid changes		SP	1.463	8.014	5.378	16.403	10.025	45.078	13.236	47.048
		BL	1.463	8.014	4.864	18.876	8.725	21.134	10.046	40.136
		TCT	1.463	8.014	2.253	10.935	5.276	12.564	4.504	12.056

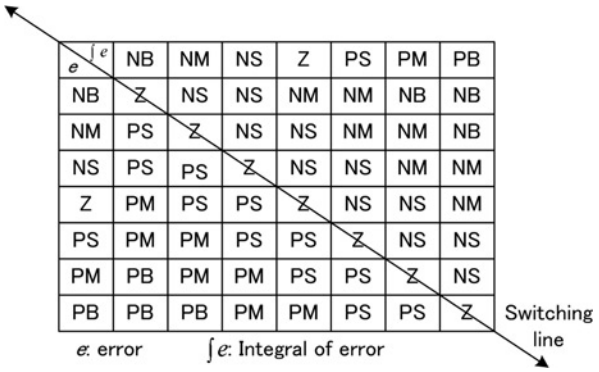

Figure 6 *Fuzzy rules assignment table*

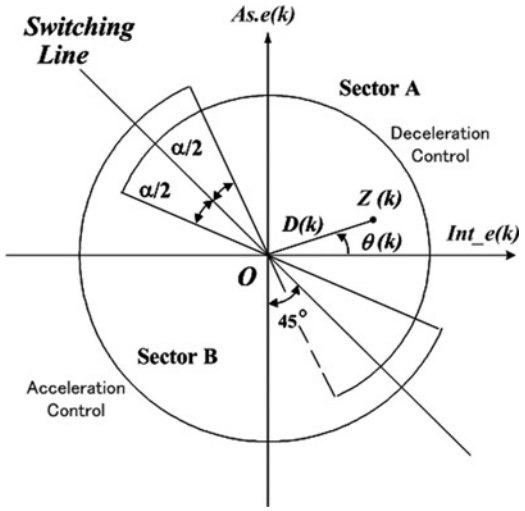

Figure 7 *Phase plane of fuzzy logic control with polar information*

the control actions in sectors which are located in the second and fourth quadrants can be stated either as deceleration or acceleration. The coordinate of the point $Z(k)$ in Fig. 7 is given by

$$Z(k) = \left[\text{Int\_}e(k), A_s e(k)\right] \tag{10}$$

where Int_$e(k)$ and $e(k)$ are the state of integral of error and error, respectively and A_s is the scaling factor of the error. Normally, the input signals of fuzzy logic controller could be error, derivative of error and integral of error. However, in this proposed method, the error and integral error are selected as input signals for two-dimensional fuzzy logic controller. The error is defined as the deviation between the estimated optimum voltage (V_{dc}^*) and controlled dc side voltage (V_{dc}). The V_{dc} itself is initially set very close to the MPP voltage (V_{mp}). By comparison with the PSS application in [14], the integral error is assumed equal to the speed deviation state, whereas the error is considered similar to the acceleration state.

The control actions in the phase plane are transformed into two membership functions during the fuzzification stage, where the linguistic variables are obtained from numerical inputs based on membership function. In this case, there are two membership functions; angle and radius membership functions. The linguistic variables in the angle membership function are the deceleration $N(\theta(k))$ and acceleration $P(\theta(k))$ control actions where their grades are shown in Fig. 8. The angle $\theta(k)$ and the radius $D(k)$ can be calculated by using state variables Int_$e(k)$ and $e(k)$ in

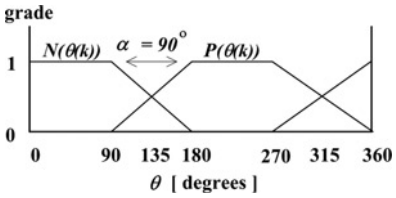

Figure 8 *Angle membership function*

Fig. 7 as follows

$$\theta(k) = \tan^{-1}\left(\frac{A_s e(k)}{\text{Int\_}e(k)}\right) \tag{11}$$

$$D(k) = \sqrt{(\text{Int\_}e(k))^2 + (A_s e(k))^2} \tag{12}$$

Meanwhile, the grade of the radius membership functions, denoted by $G(D(k))$ as shown in Fig. 9 is specified as

$$G(D(k)) = \begin{cases} \dfrac{D(k)}{D_r} & \text{for} \quad D(k) \le D_r \\ 1.0 & \text{for} \quad D(k) \ge D_r \end{cases} \tag{13}$$

where D_r is the radius member. The selected tuning parameters of A_s and D_r are specified at 5.0 and 0.35, respectively.

In the defuzzification stage, the linguistic variables are converted back to numerical variables as the fuzzy controller output based on the membership function. The fuzzy control rules always bring the current state to the equilibrium point (O) to produce the desired control signal. The control (stabilising) signal $U_c(k)$ is determined by the weighted averaging defuzzification algorithm which is formulated in (14). The established control signal will be able to keep the dc side voltage (V_{dc}) of PV system to estimated optimum voltage (V_{dc}^*) which is obtained from the ANN output.

$$U_c(k) = \frac{N(\theta(k)) - P(\theta(k))}{N(\theta(k)) + P(\theta(k))} G(D(k)) U_{max} \tag{14}$$

As the defuzzification result, the voltage control signal (U_c) will be able to maintain the operating voltage of PV array to its optimum voltage (V_{dc}^*) from ANN by applying either deceleration or acceleration controls. The control actions depend on the state of operating voltage V_{dc} to the V_{dc}^*. If the V_{dc} is suddenly increased beyond the V_{dc}^*, then the deceleration control is applied to bring back the operating value to the reference value, and vice versa. The U_c is modified into U_{CNV} by time delay about 0.05 s following the real operation, so that the V_{dc} will be always modified after this time delay setting.

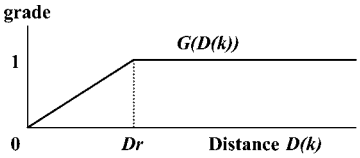

Figure 9 *Radius membership function*

3 Verification of proposed method by experimental time-accelerated real-time simulator

Since there are various possible partially shaded scenarios, it is very difficult to examine the behaviour of proposed system in real environmental conditions. On the other hand, some shadow options may give a similar effect for different configurations or one configuration has a better performance for only a specific shading scenario [15]. These factors could lead to an error for showing the proposed system performance. Thus, in this study, several inhomogeneous irradiance distributions are used to investigate the behaviour of the proposed system. In addition, since the field testing is costly, time consuming and depends heavily on the prevailing weather condition, experimental works with real-time simulator allows properly the inclusion of mismatching effects with high accuracy. With real-time simulation, not only performing analysis using real-time system parameters, what-if scenarios simply can be simulated by taking action using the online system model. The real-time simulator can also allow increasing experience of the PV system behaviour as well as an actual system. In that respects, the experimental real-time simulator is developed to verify the proposed method as shown in Fig. 10. The designer can simulate the impact of suddenly changing in irradiance on a large scale PV system or different solar cell technologies without expense by using real-time simulator. The main frame of simulator model consists of two computers with analog–digital (AD) and digital–analog (DA) hardware. The external controller is implemented on a real-time dSPACE platform. The rapid prototyping concept gives a user-friendly environment to develop some laboratory tests. The external controller receives signals and sends signals exactly as if it is connected to the real system. The dSPACE provides complete solutions for electronic control unit software development. It is powerful development tools for dedicated services in the field of function prototyping, target implementation and electronic control unit testing. Real-time control systems can be built using dSPACE and the control logic can be implemented. The dSPACE works on

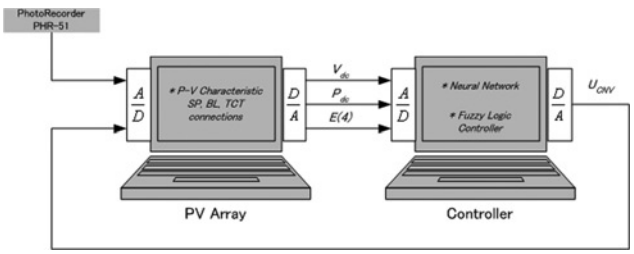

Figure 10 *Configuration of real-time simulator*

doi: 10.1049/iet-rpg:20080065

Matlab/Simulink platform which is a common engineering software and easy to understand and obtain experience without expense and time consuming.

The experimental time-accelerated real-time simulator is divided into two main parts, that is, outdoor and indoor equipments. The outdoor equipment is the PhotoRecorder PHR-51, whereas two PCs which are embedded with AD/DA hardware are classified as indoor equipment. The PhotoRecorder PHR-51 is basically working following the silicon solar cell principal to measure the light intensity, which is in Lux unit. To obtain the irradiance measurement, a unit conversion is required, where 1 Lux is equal to 0.0161028 W/m^2. This irradiance measurement (E) can be either directly transferred to the PV array computer using USB cable of RSAQ5R or through the A/D converter. In the indoor equipment, the setting of real-time simulator is configured based on two simulation software environments. Initially, the overall system configuration is set for digital simulation by using Matlab/Simulink ver. 6.5. Then, this program is compiled using software dSPACE real-time interface (RTI) ver.5.0 for analog or real-time simulation. The simulation is performed in time-accelerated mode, means 1 s in the simulation can represent 1 h in the real-time practice. The voltage signal margin about 10 V is used for AD and DA hardware.

In Fig. 10, the PV array system with SP, BL and TCT array configurations is set up inside the first computer, whereas the ANN and fuzzy logic controller properties are set up in the second computer. The first computer behaves as PV array system where the P–V curve can be observed as the output following the variation in irradiance level (E) and cell temperature (T_c). To determine the shading patterns for 3 × 3 PV array; 4 irradiance measurements, denoted by $E(4)$ is intentionally generated in the first computer. These signals are the main input for the ANN signal processing in the second computer. The real-time simulator works continuously by sending these irradiance signals, together with P_{dc} and V_{dc} through the coaxial cable of RG-58c/u from the first computer to the second computer which behaves as controller unit to produce control signal (U_{CNV}) that is always fed back to the first computer. The V_{dc} and P_{dc} are also initially set very close to the MPP voltage and power. Owing to the control actions, the controlled voltage (V_{dc}) is always modified for every 0.05 s following the real operation of PV system and DC–DC converter.

The proposed real-time simulator configuration can be also called as virtual PV system with MPPT controller. The simulator can be utilised for evaluation of the MPPT controller on different types of PV system, with different scenarios, even without having the PV module hardware.

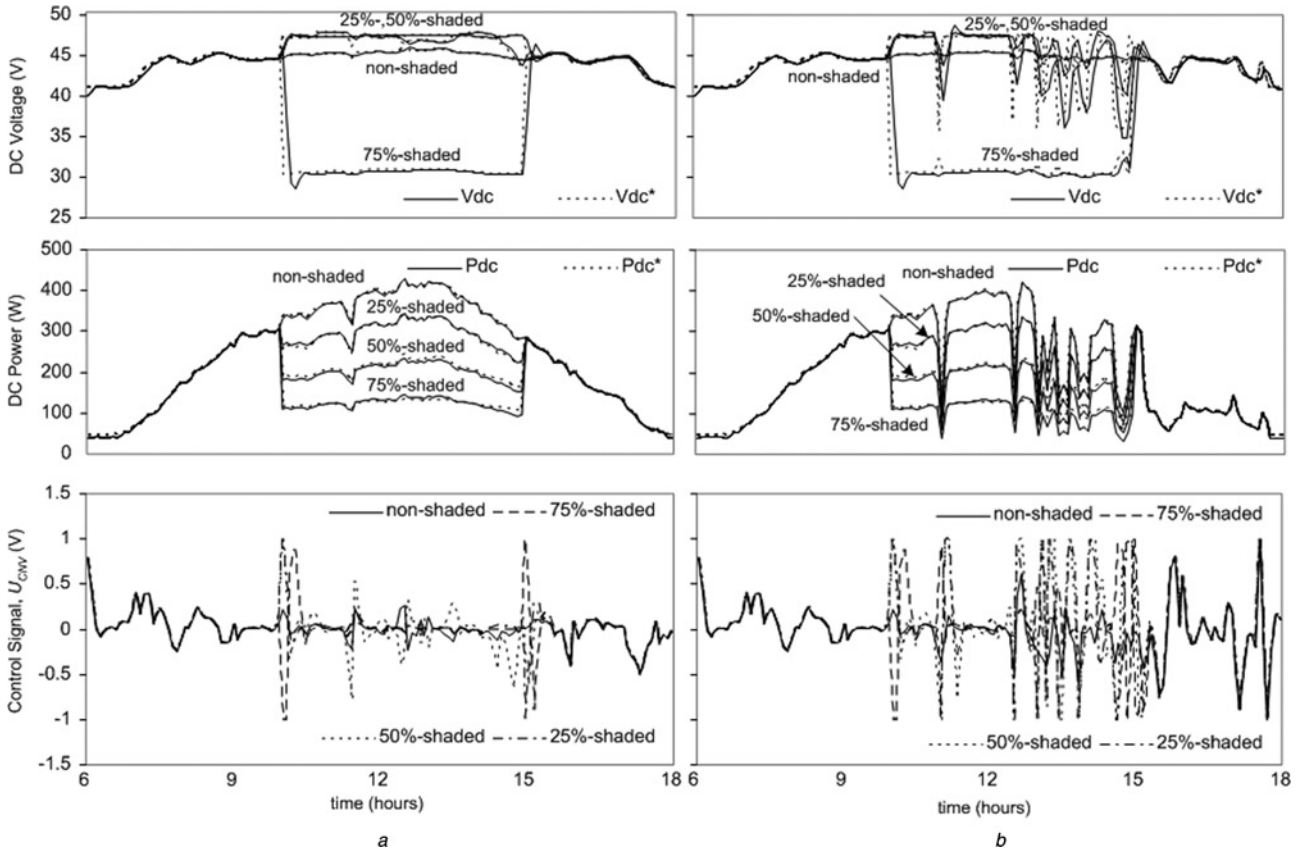

Figure 11 *DC Voltage, MPPT and control signal of SP connection with 5M shaded for 3 × 3 PV array*

a Slow changes in irradiance
b Rapid changes in irradiance

As a result, the simulator will be very simple and useful to several cases for evaluating a proposed PV system for special environmental conditions such as partial shading. The verification outputs in real-time simulator with analog signal shows similar results from digital simulation (Matlab/Simulink) since there are no deformation signals transfers between PV array and controller computers.

The proposed method is tested for six different PV array connections with given irradiance profiles in Fig. 4. The terms of 75%-shaded, 50%-shaded and 25%-shaded mean that the irradiation of selected modules are reduced by 75%, 50% and 25%, respectively according to the irradiation of non-shaded modules. The shaded modules are specified as 1M, 5M and 8M. For instance, 5M means that the shade covers from module-1 to module-5. Different partially shaded scenarios are created arbitrarily between 10 a.m. and 3 p.m., during that duration irradiance of PV array reaches peak levels.

To show the performance of the proposed method, the SP connection with shaded PV modules form M1 to M5 is investigated in 3 × 3 PV array. This shading pattern can be considered as moderately shaded conditions for 3 × 3 PV array. In that case, three peaks occur on the $P–V$ curve. For 75%-shaded case, the optimum voltage is shifted from 40 V to 30 V and the optimum power reduces significantly. It is clearly shown in Fig. 11 that the PV array can be operated at the optimum voltage by following the ANN output for all shading conditions.

In the second case, M1 is shaded with 25%, 50% and 75% in 3 × 3 BL configurations. This shading pattern can be considered as lightly shaded conditions because of the small area of array faces the shadow condition. Consequently, output power reduces less significant and optimum voltage is remained in the normal MPP voltage that is under non-shaded insolation condition. As can be seen in Fig. 12, the proposed method is working very well for all shading conditions.

The third case is about the performance of the proposed method on the TCT configuration with shaded PV modules from M1 to M8 in 3 × 3 PV array. Although this shading pattern can be classified as heavily shaded condition, the operating voltage is not changed in a large voltage window. However, the output power is significantly reduced. Under this scenario, the characteristic of PV array is almost the same as that of the very low uniform insolation condition. Fig. 13 presents the effectiveness of proposed method to operate the PV array at optimum voltage for all shading conditions.

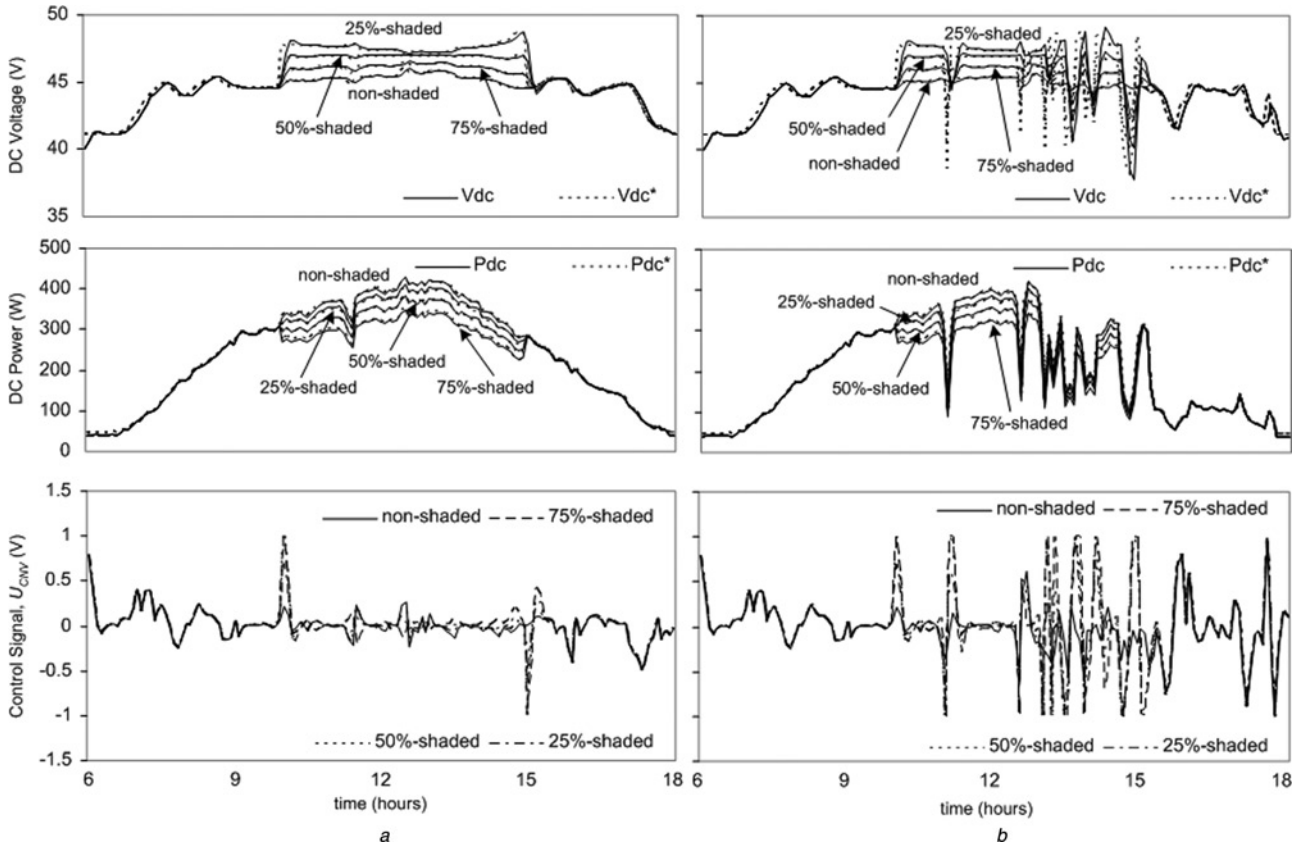

Figure 12 *DC Voltage, MPPT and control signal of BL connection with 1M shaded for 3 × 3 PV array*

a Slow changes in irradiance
b Rapid changes in irradiance

IET Renew. Power Gener., 2009, Vol. 3, Iss. 2, pp. 239–253
doi: 10.1049/iet-rpg:20080065

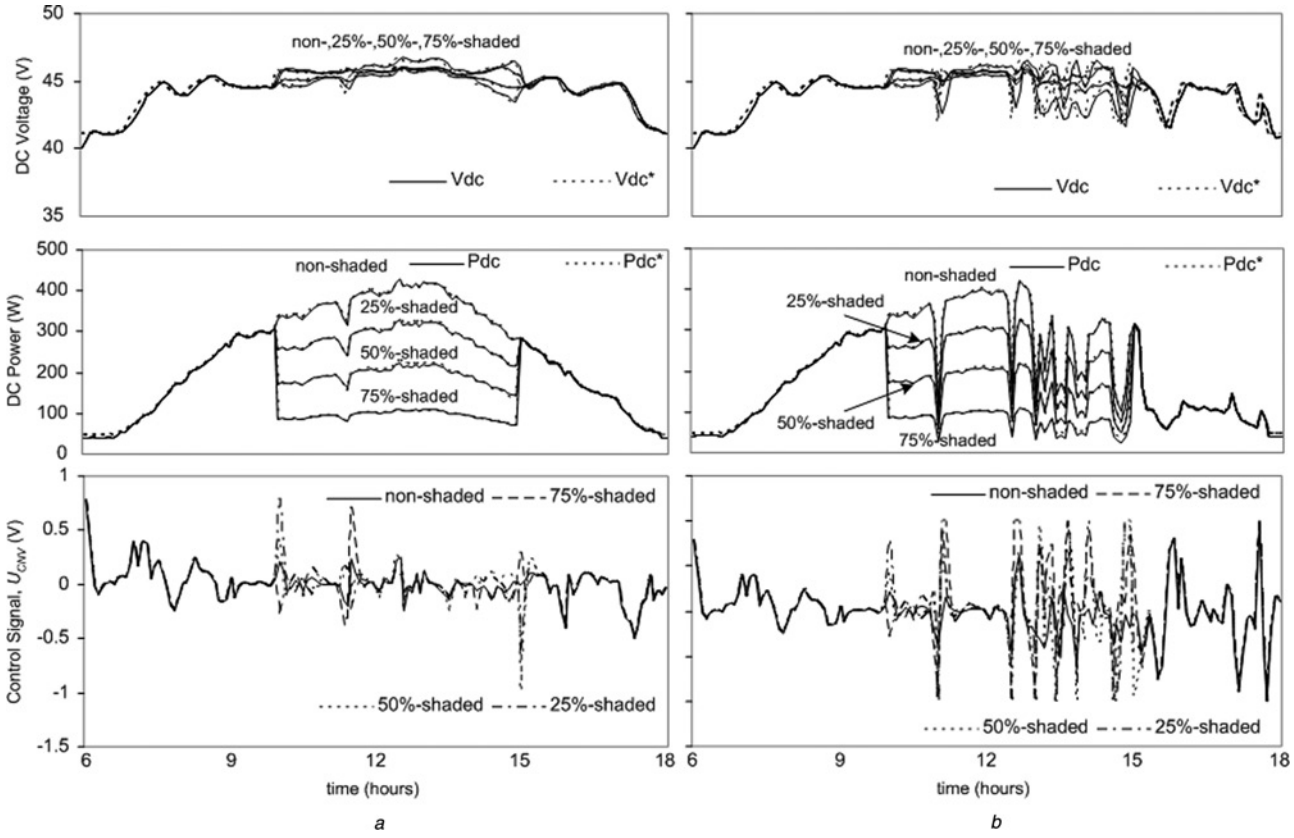

Figure 13 *DC Voltage, MPPT and control signal of TCT connection with 8M shaded for 3 × 3 PV array*

a Slow changes in irradiance
b Rapid changes in irradiance

The overall results in the control responses are again measured by a performance index, denoted by J_{cont} in order to convince on how close the results between the dc control voltage (V_{dc}) and the optimum voltage (V_{dc}^{*}). This index is simply formulated in (15) and the performance index results for 3 × 3 PV array is presented in Table 4.

$$J_{cont} = \int (V_{dc}^{*} - V_{dc})^2 \, dt \tag{15}$$

Table 4 Performance index of the proposed controller (J_{cont}) for 3 × 3 PV array

Irradiance	PV array	Non-shaded	25%-shaded	50%-shaded	75%-shaded
Slow changes	SP	0.493	1.131	2.406	16.501
	BL	0.493	0.592	0.948	1.729
	TCT	0.493	0.597	0.798	0.814
Rapid changes	SP	2.057	9.239	13.846	20.178
	BL	2.057	5.462	10.655	13.337
	TCT	2.057	2.778	7.216	4.893

In the fourth case, the reliability of proposed system is tested for 20 × 3 in all PV array configurations. Table 5 shows the performance comparison between conventional perturbation–observation (P&O) method [2] and the proposed MPPT system in actual time practice. As can be seen easily, the proposed system has higher efficiency than the conventional method in terms of output power of PV arrays. The overall results show that the proposed method can be used to track the global MPP of small and large size PV arrays under non-uniform insolation conditions.

4 ANN based estimated energy generation of PV system under partially shaded conditions

Another benefit of this proposed method is the ability to predict the maximum energy generation of PV system, even under partially shaded condition. The estimated maximum energy production (W_{dc}^{*}) of PV system are determined by using the ANN output power. The real-time simulation results based on the estimation maximum energy production for 3 × 3 PV array is presented in Fig. 14. Similar to the voltage controller performance index, the

Table 5 V_{dc} and P_{dc} outputs of 20 × 3 array configuration under partially shaded conditions

Time (h)	Shading patterns on modules area (W/m^2)				SP				BL				TCT			
					P&O		Proposed controller		P&O		Proposed controller		P&O		Proposed controller	
	A	B	C	D	V_{dc} (V)	P_{dc} (W)	V_{dc} (V)	P_{dc} (W)	V_{dc} (V)	P_{dc} (W)	V_{dc} (V)	P_{dc} (W)	V_{dc} (V)	P_{dc} (W)	V_{dc} (V)	P_{dc} (W)
10.00	250	150	250	750	320.60	485.66	223.32	546.33	320.60	486.69	227.74	554.85	320.60	486.84	227.74	555.47
10.30	150	500	750	750	340.50	514.65	236.58	1179.40	340.50	514.66	236.58	1180.60	340.50	514.67	236.58	1181.00
11.00	500	750	1000	1000	333.87	1683.30	234.37	1747.30	333.87	1683.30	234.37	1748.50	333.87	1683.40	234.37	1748.96
11.30	250	500	750	1000	338.29	854.30	238.79	1199.80	338.29	854.38	238.79	1201.50	338.29	854.43	238.79	1201.90
12.00	500	250	500	750	331.66	835.98	223.32	1089.00	331.66	837.49	225.53	1095.30	331.66	837.73	225.53	1103.00
12.30	150	500	150	500	313.97	465.73	139.30	663.79	313.97	465.73	139.30	663.79	313.97	465.73	139.30	663.79
1.00	500	750	150	250	329.45	499.30	150.35	737.26	329.45	499.33	148.14	728.20	329.45	499.35	148.14	727.79
1.30	750	500	250	500	331.66	838.50	227.74	1107.30	331.66	838.50	227.74	1107.30	331.66	838.50	227.74	1107.30
2.00	1000	750	500	250	338.29	856.99	241.01	1213.40	338.29	856.70	241.01	1212.90	338.29	856.28	241.01	1203.50
2.30	1000	1000	750	500	333.87	1688.10	236.58	1767.50	333.87	1687.70	236.58	1766.00	333.87	1686.90	234.37	1751.60
3.00	750	750	150	150	320.60	476.33	143.72	1014.80	320.60	476.07	141.51	999.55	320.60	475.71	141.51	999.51

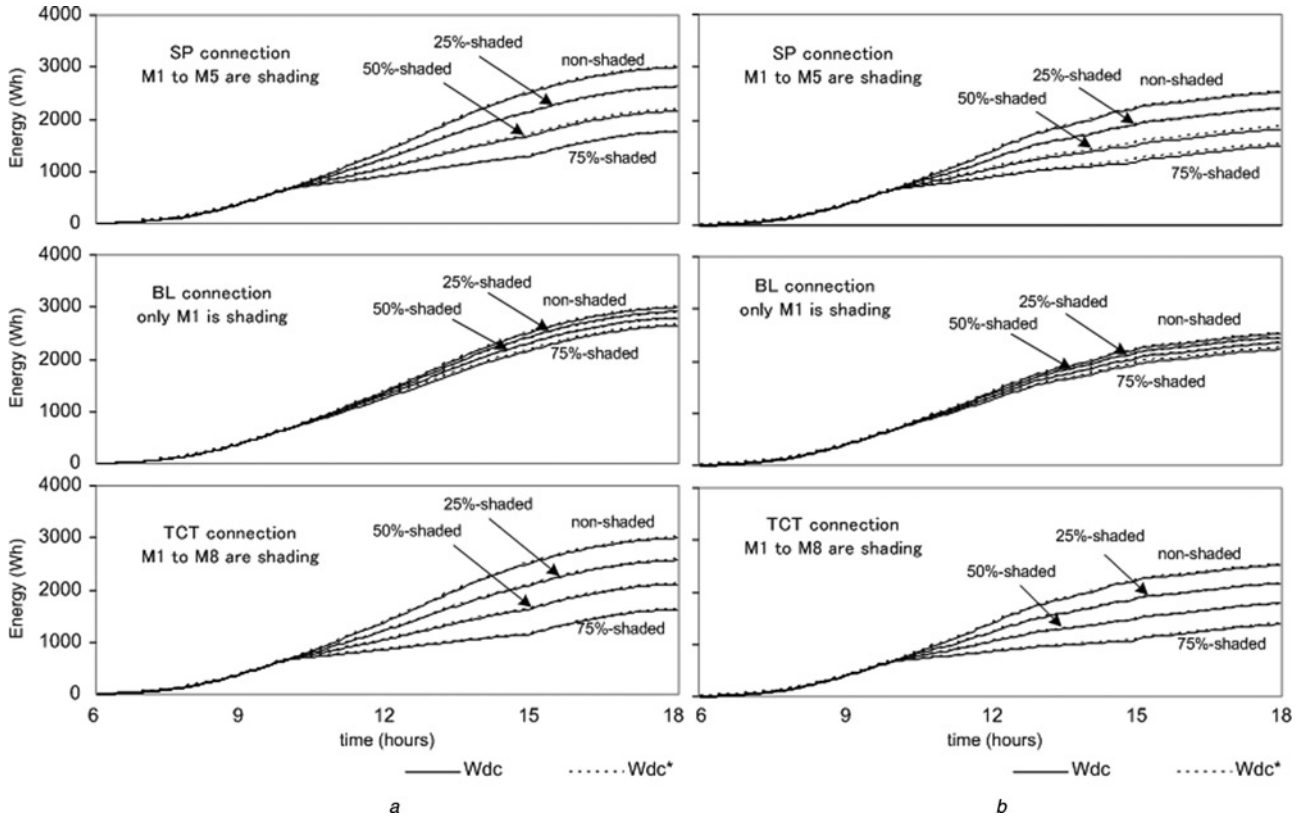

Figure 14 *Estimation of maximum energy production of PV array under partially shaded conditions for 3 × 3 PV array*

a Slow changes in irradiance
b Rapid changes in irradiance

energy performance index (J_E) is also introduced based on (16) to show the differences between the actual maximum energy production (W_{dc}) and the estimated maximum energy production (W^*_{dc}). The results of J_E for the 3 × 3 PV array are shown in Table 6

$$J_E = \int (W^*_{dc} - W_{dc})^2 \, dt \tag{16}$$

doi: 10.1049/iet-rpg:20080065

Table 6 Performance index between estimated energy and actual energy (J_E) for 3 × 3 PV array

Irradiance	PV array	Non-shaded	25%-shaded	50%-shaded	75%-shaded
Slow changes	SP	15.828	53.280	68.340	14.836
	BL	15.828	45.500	50.330	67.445
	TCT	15.828	15.549	19.293	23.629
Rapid changes	SP	19.030	38.433	39.880	28.505
	BL	19.030	46.520	48.836	50.705
	TCT	19.030	15.012	18.292	16.128

The same method of energy prediction under partially shaded condition is then applied for the 20 × 3 PV systems. The real-time simulation of energy estimation for this PV system under the shading patterns in the A, B, C, D regions is shown in Table 7.

As the output power decreases under the shading condition, the energy production is consequently also reduced. Fig. 14 and Table 7 are enough to explain the reduction of energy estimation for the small size and large size of PV system under partially shaded conditions. In Fig. 14, significant drop in the cumulative energy estimation can be caused either by wide area of shading or heavily reduced intensity of sunlight. In these results, 5 modules and 8 modules are shading in the SP and TCT connections, respectively with reducing 75% of light intensity will proceed about a-half reduction in the energy estimation for 3 × 3 PV array. Similar trends occur in the large size of PV system. Shading patterns in the regions A, B, C and D in 20 × 3 PV array yield almost a-half of energy reduction, compared with the same period of non-shaded condition, especially when the actual irradiance condition is good and its changes are slowly. The overall results in both cases are based on deploying the explained control topology. Much remarkable energy reduction will occurs without applying the control method. Therefore, obtaining more energy under the shading conditions can be the challenge of the planning, operation and decision making in solar energy investment.

Estimation of output power and energy of PV systems in the planning operation is very important since the output of the PV system depends on the environmental condition. Some benefits can be obtained by predicting the maximum power and energy of PV system early. There are two common operations of PV system in the grid, either in the form of stand-alone or hybrid systems. In the stand-alone and hybrid PV systems, the estimated output power will be very useful to optimise the operation of equipment, such as battery and inverter. The optimised operation of battery in this case is related to the accuracy of charging and discharging schedules in order to prolong the life time of the battery and to reduce the low-load engine operation. In terms of inverter operation, the prediction of the inverter output can be done since the inverter efficiency is the function of output power of PV system.

Another advantage of predicting the output power of PV system in the hybrid operation is the availability of accurate

Table 7 Accumulative energy estimation of 20 × 3 PV array

Time (h)	Estimated energy in non-shaded condition (kWh)		Shading patterns on modules area (W/m2)				Estimated energy under shaded condition (kWh)					
							SP		BL		TCT	
	Slow changes	Rapid changes	A	B	C	D	Slow changes	Rapid changes	Slow changes	Rapid changes	Slow changes	Rapid changes
10.00	4.563	4.415	250	150	250	750	4.148	4.000	4.150	4.002	4.150	4.002
10.30	5.667	5.519	150	500	750	750	4.579	4.431	4.584	4.436	4.584	4.436
11.00	6.834	6.260	500	750	1000	1000	5.311	5.163	5.316	5.168	5.317	5.169
11.30	8.078	7.078	250	500	750	1000	6.048	5.900	6.054	5.906	6.055	5.907
12.00	9.366	8.366	500	250	500	750	6.620	6.472	6.628	6.480	6.631	6.483
12.30	10.740	9.287	150	500	150	500	7.058	6.910	7.068	6.920	7.073	6.924
1.00	12.156	9.774	500	750	150	250	7.409	7.260	7.416	7.268	7.420	7.272
1.30	13.508	10.282	750	500	250	500	7.870	7.722	7.875	7.727	7.879	7.731
2.00	14.767	10.857	1000	750	500	250	8.450	8.302	8.455	8.307	8.457	8.309
2.30	15.906	11.679	1000	1000	750	500	9.195	9.047	9.199	9.051	9.196	9.048
3.00	16.910	12.732	750	750	150	150	9.891	9.743	9.891	9.743	9.883	9.735

scheduling for other units of generation, for instance the diesel engine and hydro power. Accurate prediction and coordination between units will improve the supply reliability and reduce the cost investment. At the end of the day, the estimated output power of PV system in hybrid system will contribute to reduce the fuel consumption, to optimise the number of operating hours and to reduce the maintenance cost for other generation units.

Similar to the benefits of predicting the output power, the estimated output energy of PV system can be beneficial to determine the estimated electricity tariff in certain power grid. The electricity cost which is measured in currency/kWh can be estimated as money saving when the PV system is connected to the grid. Moreover, the benefits of solar energy investment which is specified as gain or loss can be figured out by using information of estimated output energy.

5 Conclusion

The effectiveness of the proposed neuro-fuzzy schemes for the MPPT control and the prediction of maximum energy generation of PV system under partially shaded conditions have been presented. Since the optimum MPP voltage and power are directly obtained by using ANN, the proposed system does not need complex algorithms and advanced power electronic control units. The results show that the ANN is sufficiently accurate in mapping between a partially shaded condition and optimum voltage and power of a PV array. The fuzzy logic control with polar information is deployed to keep the operating voltage of PV system at optimal point. In addition to this, the same ANN structure can also be used to estimate maximum energy generation of PV system under partially shaded conditions. The proposed system has been verified through the experimental real-time simulator for different size of PV array with SP, BL and TCT configurations. The conventional MPPT systems stop at the first local MPP and may not scan the power–voltage curve for the global MPP. The proposed system enables to guarantee the operation at global MPP. Through the all results presented show more power can be extracted and overall energy yield can be increased with the proposed system under from lightly to heavily partially shaded conditions.

6 References

[1] ROMAN E., ALONSO R., IBANEZ P.: 'Intelligent PV module for grid-connected PV systems', *IEEE Trans. Ind. Electron.*, 2006, **53**, (4), pp. 1066–1073

[2] ESRAM T., CHAPMAN P.L.: 'Comparison of photovoltaic array maximum power point tracking techniques', *IEEE Trans. Energy Convers.*, 2007, **22**, (2), pp. 439–449

[3] HOHM D.P., ROPP M.E.: 'Comparative study of maximum power point tracking algorithms', *Prog. Photovolt., Res. Appl.*, 2003, **11**, (1), pp. 47–62

[4] KARATEPE E., HIYAMA T., BOZTEPE M., COLAK M.: 'Voltage based power compensation system for photovoltaic generation system under partially shaded insolation conditions', *Energy Convers. Manage.*, 2008, **49**, (8), pp. 2307–2316

[5] WOYTE A., NIJS J., BELMANS R.: 'Partial shadowing of photovoltaic arrays with different system configurations: literature review and field test results', *Sol. Energy*, 2003, **74**, (3), pp. 217–233

[6] SOLODOVNIK E.V., LIU S., DOUGAL R.A.: 'Power controller design for maximum power tracking in solar installations', *IEEE Trans. Power Electron.*, 2004, **19**, (5), pp. 1295–1304

[7] SHIMIZU T., HIRAKATA M., KAMEZAWA T., WATANABE H.: 'Generation control circuit for photovoltaic modules', *IEEE Trans. Power Electron.*, 2001, **16**, (3), pp. 293–300

[8] MISHIMA T., OHNISHI T.: 'A power compensation strategy based on electric double layer capacitors for partially shaded PV array'. Proc. Fifth PEDS Int. Conf., Singapore, November 2003, pp. 858–863

[9] KOBAYASHI K., TAKANO I., SAWADA Y.: 'A study of a two-stage maximum power point tracking control of a photovoltaic system under partially shaded insolation conditions', *Electr. Eng. Jpn*, 2005, **153**, (4), pp. 39–49

[10] IRISAWA K., SAITO T., TAKANO I., SAWADA Y.: 'Maximum power point tracking control of photovoltaic generation system under nonuniform insolation by means of monitoring cells'. Proc. 28th IEEE Photovoltaic Specialists Conf., Alaska, USA, September 2000, pp. 1707–1710

[11] AHMED N.A., MIYATAKE M.: 'A novel maximum power point tracking for photovoltaic applications under partially shaded insolation conditions', *Electr. Power Syst. Res.*, 2008, **78**, (5), pp. 777–784

[12] PATEL H., AGARWAL V.: 'MATLAB-based modeling to study the effects of partially shaded on PV array characteristics', *IEEE Trans. Energy Convers.*, 2008, **23**, (1), pp. 302–310

[13] PATEL H., AGARWAL V.: 'Maximum power point tracking scheme for PV systems operating under partially shaded conditions', *IEEE Trans. Ind. Electron.*, 2008, **55**, (4), pp. 1689–1698

[14] HIYAMA T.: 'Fuzzy logic power system stabilizer using polar information' in El-Hawary M.E. (Ed.): 'Electric power applications of fuzzy systems' (IEEE Press, 1998, 2nd edn.), pp. 149–177

[15] KARATEPE E., BOZTEPE M., COLAK M.: 'Development of a suitable model for characterizing photovoltaic arrays with shaded solar cells', *Sol. Energy*, 2007, **81**, (8), pp. 977–992

doi: 10.1049/iet-rpg:20080065

[16] GABLER H.: 'Autonomous power supply with photovoltaics: photovoltaics for rural electrification: reality and vision', *Renew. Energy*, 1998, **15**, (1–4), pp. 512–518

[17] BOWER W., DEBLAISO R.: 'Code requirements and standards for installations of photovoltaic systems in the US', *Prog. Photovolt., Res. Appl.*, 1999, **7**, (3), pp. 155–164

[18] MAISH A.: 'Defining requirements for improved photovoltaic system reliability', *Prog. Photovolt., Res. Appl.*, 1999, **7**, (3), pp. 165–173

[19] ABDULLAH A.H., GHONEIM A.A., AL-HASAN A.Y.: 'Kuwaiti assessment of grid-connected photovoltaic systems in Kuwaiti climate', *Renew. Energy*, 2002, **26**, (2), pp. 189–199

[20] MONDOL J.D., YOHANIS Y.G., NORTON B.: 'Comparison of measured and predicted long term performance of grid a connected photovoltaic system', *Energy Convers. Manage*, 2007, **48**, (4), pp. 1065–1080

[21] BILLINTON R., BAGEN : 'Generating capacity adequacy evaluation of small stand-alone power systems containing solar energy', *Reliab. Eng. Syst. Saf.*, 2006, **91**, (4), pp. 438–443

[22] HIYAMA T., KITABAYASHI K.: 'Neural network based estimation of maximum power generation from PV module using environmental information', *IEEE Trans. Energy Convers.*, 1997, **12**, (3), pp. 241–247

[23] http://www.shell.com/renewables, accessed July 2007

[24] SYAFARUDDIN, HIYAMA T., KARATEPE E.: 'Identification of shading patterns of photovoltaic array through the *P–V* characteristic measurements'. Proc. First Student Int. Conf. Advanced Science and Technology, Kumamoto, Japan, March 2008, pp. 153–154

[25] ALONSO-GARCIA M.C., RUIZ J.M., CHENLOA F.: 'Experimental study of mismatch and shading effects in the I–V characteristic of a photovoltaic module', *Sol. Energy Mater. Sol. Cells*, 2006, **90**, (3), pp. 329–340

[26] KAJIHARA A., HARAKAWA A.T.: 'Model of photovoltaic cell circuits under partial shading'. Proc. IEEE Int. Conf. Industrial Technology, Hong Kong, December 2005, pp. 866–870

[27] KING D.L., BOYSON W.E., KRATOCHVIL J.A.: 'Photovoltaic array performance model'. SAND2004-3535, Sandia National Laboratories, August 2004

[28] DRIESSE A., HARRISON S., JAIN P.: 'Evaluating the effectiveness of maximum power point tracking methods in photovoltaic power systems using array performance models'. Proc. Power Electronics Specialists Conf. (PESC), Florida, USA, June 2007, pp. 145–151

[29] HIYAMA T., KOUZUMA S., IMAKUBO T.: 'Identification of optimal operating point of PV modules using neural network for real-time maximum power tracking control', *IEEE Trans. Energy Convers.*, 1995, **10**, (2), pp. 360–367